Earth and Planetary Science Letters 500 (2018) 117–126

Contents lists available at ScienceDirect

Earth and Planetary Science Letters

www.elsevier.com/locate/epsl

# Pervasive aerobic nitrogen cycling in the surface ocean across the Paleoproterozoic Era

Michael A. Kipp [a,b,*], Eva E. Stüeken [b,c], Misuk Yun [d], Andrey Bekker [e,f], Roger Buick [a,b]

[a] Department of Earth & Space Sciences and Astrobiology Program, University of Washington, Seattle, WA 98195, USA
[b] Virtual Planetary Laboratory, NASA Astrobiology Institute, Seattle, WA 98195, USA
[c] School of Earth & Environmental Sciences, University of St. Andrews, KY16 9AL, Scotland, United Kingdom
[d] Department of Geological Sciences, University of Manitoba, Winnipeg, Manitoba, R3G 2K4 Canada
[e] Department of Earth Sciences, University of California, Riverside, CA 92521, USA
[f] Department of Geology, University of Johannesburg, P.O. Box 524, Auckland Park, 2006, Republic of South Africa

ARTICLE INFO

*Article history:*
Received 14 March 2018
Received in revised form 2 August 2018
Accepted 4 August 2018
Available online xxxx
Editor: D. Vance

*Keywords:*
Paleoproterozoic
nitrogen isotopes
paleoredox
eukaryote evolution
Great Oxidation Event
Lomagundi Event

ABSTRACT

Nitrogen isotope ratios in marine sedimentary rocks have become a widely used biogeochemical proxy that records information about nutrient cycling and redox conditions in Earth's distant past. While the past two decades have seen considerable progress in our understanding of the Precambrian sedimentary nitrogen isotope record, it is still compromised by substantial temporal gaps. Furthermore, quantitative links between nitrogen isotope data, marine redox conditions, and nutrient availability are largely lacking in a Precambrian context. Here we present new nitrogen isotope data from a suite of marine sedimentary rocks with ca. 2.4 to 1.8 Ga ages, spanning the Great Oxidation Event in the Paleoproterozoic, to better constrain the response of the nitrogen cycle to the first major redox transition in Earth's history. We further construct a simple box model to describe the major pathways that influenced the nitrogen isotope mass balance of the Precambrian ocean and use this as a platform to evaluate the Precambrian nitrogen isotope record. Within this framework, we find that consistently positive nitrogen isotope values, ranging from +1.1 to +7.7‰, across the early Paleoproterozoic are strong evidence for an expansion of oxygenated surface waters. Since the isotopic signature of aerobic nitrogen cycling is recorded in the biomass of nitrate-assimilating organisms, this implicates widespread nitrate bioavailability in this time interval. The decline in offshore nitrogen isotope ratios in the Mesoproterozoic is consistent with the contraction of oxic waters, which could have inhibited the expansion of nitrate-fueled ecosystems to pelagic waters until the widespread oxygenation of the ocean in the latest Neoproterozoic to early Phanerozoic.

© 2018 Elsevier B.V. All rights reserved.

## 1. Introduction

At the beginning of the Paleoproterozoic Era, Earth's atmosphere underwent a permanent shift from a reducing to an oxidizing state. This transition – termed the "Great Oxidation Event" (GOE) – began by ca. 2.43 Ga (Gumsley et al., 2017) and was characterized by oxygen-rich marine and terrestrial settings lasting until ca. 2.06 Ga (Bekker and Holland, 2012). In the aftermath of the GOE, atmospheric oxygen fell to an intermediate level that was substantially higher than in the Archean, but lower than Phanerozoic concentrations (Lyons et al., 2014). While the exact timing and mechanism of the GOE remain debated, the magnitude of its implications is clear: the biogeochemical pathways operating at Earth's surface were dramatically and permanently altered (Lyons et al., 2014), and the stage was set for the emergence of aerobically-respiring organisms, including the first eukaryotes (Javaux and Lepot, 2018).

Several paleo-redox proxies have been used to characterize the transition toward oxygenated surface environments in the Paleoproterozoic. Early evidence from oxidized paleosols documented the influence of atmospheric oxygen in weathering environments by ca. 2.2 Ga (e.g. Beukes et al., 2002), and the recognition of a large perturbation in the global carbon cycle through carbon isotope systematics of carbonates has long been used to support a notion of extreme oxygen production during the GOE (e.g. Karhu and Holland, 1996). More recently, the disappearance of mass-independent fractionation of sulfur isotopes (MIF-S) has been used to pinpoint the crossing of a threshold of $10^{-5}$ times the present

* Corresponding author at: Johnson Hall Room 070, Dept. of Earth & Space Sciences, University of Washington, 4000 NE 15th Ave, Seattle, WA 91895-1310, USA.
*E-mail address:* kipp@uw.edu (M.A. Kipp).

https://doi.org/10.1016/j.epsl.2018.08.007
0012-821X/© 2018 Elsevier B.V. All rights reserved.

atmospheric level of oxygen (PAL) between 2.46 and 2.32 Ga (Farquhar et al., 2000; Gumsley et al., 2017; Luo et al., 2016; Bekker et al., 2004), which has come to define the onset of the GOE proper.

The redox states of the atmosphere and ocean are coupled on geologic timescales, and so the rise of atmospheric oxygen, the "oxygen overshoot," and the subsequent deoxygenation should have considerably affected marine redox chemistry. Indeed, enrichments of redox-sensitive trace elements in organic-rich shales implicate an expansion of oxygenated seawater during the GOE (Scott et al., 2008; Partin et al., 2013; Kipp et al., 2017), as do sulfur isotope ratios in marine sedimentary rocks, which suggest a waxing and waning seawater sulfate reservoir (Planavsky et al., 2012; Scott et al., 2014). Beyond these converging lines of evidence for widespread ocean oxygenation during the GOE, recent work has begun to decipher even regional redox gradients. Highly positive selenium isotope ratios in offshore marine sediments during the GOE imply oxygenated surface oceans, with anoxia prevailing at depth (Kipp et al., 2017). This finding is corroborated by the record of iodine enrichment in shallow-marine carbonates deposited at the same time, which requires at least mildly oxygenated surface waters (Hardisty et al., 2017).

Nitrogen isotope geochemistry can bring additional perspective to bear on the question of basinal redox structure, as nitrogen has a high redox potential – similar to that of selenium and iodine – and is sensitive to redox conditions in the photic zone, where primary productivity is highest. The nitrogen isotope composition of organic matter in offshore marine sediments can thus speak to redox chemistry in the photic zone overlying the outer shelf and open ocean. Furthermore, as nitrogen is an essential macronutrient, nitrogen isotopes in marine sediments also record the balance between nitrogen-fixing organisms (strictly prokaryotic) and nitrogen-assimilating organisms (which can be either prokaryotic or eukaryotic). Since nitrate ($NO_3^-$) is the preferred nitrogenous substrate for eukaryotes in the modern ocean (e.g. Karl et al., 2001), tracing the prevalence of aerobic nitrogen cycling during the Paleoproterozoic can both constrain redox conditions and speak directly to the bioavailability of $NO_3^-$ for eukaryotic organisms.

Notably, despite the wealth of evidence from a variety of well-established paleo-redox proxies, the immediate response of the nitrogen cycle to the GOE has only been investigated in a few studies that focused specifically on the onset, culmination, or aftermath of the GOE (Kump et al., 2011; Luo et al., 2018; Papineau et al., 2009; Zerkle et al., 2017). While those studies have provided important evidence for the presence of aerobic nitrogen cycling during the GOE, the sparse record through the Paleoproterozoic hinders reconstructions of global temporal and spatial patterns across the proposed "oxygen overshoot."

Here we present nitrogen isotope data from a suite of Paleoproterozoic marine sedimentary rocks that span the GOE in order to better characterize the response of the biogeochemical nitrogen cycle to the first permanent increase in atmospheric and marine oxygen levels. Taking this a step further, we then construct a simple steady-state isotope box model and use it as a platform for evaluating secular trends in the Precambrian nitrogen isotope record. To date, nitrogen isotopes in ancient marine sediments have been used at best as a semi-quantitative redox proxy. We find that even with this simple view of the nitrogen cycle, a robust correlation can be drawn between nitrogen isotope ratios in marine sediments and the extent of oxic surface waters. This new, quantitative framework for interpreting the nitrogen isotope record enables a direct comparison with results from other proxies, thereby refining our view of ocean oxygenation during and after the GOE.

## 2. Materials

We collected nitrogen and organic carbon isotopic data from a large sample set ($n = 144$) of marine, siliciclastic sedimentary rocks with ages spanning ca. 2.4 to 1.8 Ga. We targeted shales deposited in offshore depositional environments (below wave base) in basins that were open with respect to exchange with the global ocean. When viewed together, these lithologies capture a representative view of secular trends in global nitrogen cycling. None of the units studied here have experienced metamorphism beyond lower greenschist facies. Detailed descriptions of individual units can be found in the Supplementary Materials.

## 3. Methods

### 3.1. Sample preparation for bulk rock analyses

Sample preparation followed published methods (Stüeken, 2013; Koehler et al., 2017). Samples were crushed into centimeter-sized chips, and equipment was cleaned between samples with methanol and 18 MΩ DI–$H_2O$. Rock chips were sequentially cleaned with ethanol, 2 N HCl, and DI–$H_2O$ to remove modern contaminants, then dried in an oven at 60 °C. Clean chips were pulverized using an aluminum oxide puck mill that was cleaned between samples using methanol, DI–$H_2O$, and pre-combusted (500 °C) silica sand. Prior to analysis, powders were decarbonated using 6 N HCl, then rinsed with DI–$H_2O$ and dried in an oven at 60 °C.

### 3.2. Kerogen extraction

Kerogen was extracted from bulk rock powders following published protocols (Stüeken et al., 2015). Rock powders were weighed out into teflon bottles and treated with a 50:50 mixture of DI–$H_2O$ and concentrated (29 N) hydrofluoric acid (HF) in a shaking water bath at 55 °C. Digests were then centrifuged and the supernatant was decanted. A $BF_3$ solution (62.5 g $H_3BO_3$, 100 mL DI–$H_2O$, 100 mL 29 N HF) was then added, and the samples were placed in a shaking water bath at 55 °C to dissolve remaining fluoride minerals. Samples were then centrifuged, the supernatant was decanted, and the samples were washed with three iterations of DI–$H_2O$. The isolated kerogen was transferred to a combusted pyrex vial in DI–$H_2O$ and freeze-dried to remove all moisture prior to analysis.

### 3.3. Isotopic analyses

The isotopic composition ($\delta^{15}N$ and $\delta^{13}C_{org}$) of decarbonated powders and kerogen isolates was measured on a Costech™ ECS 4010 Elemental Analyzer coupled to a Thermo Finnigan™ MAT253 continuous flow isotope-ratio mass spectrometer housed in IsoLab at the Department of Earth & Space Sciences, University of Washington. Combustion was carried out with 20 ml $O_2$ at 1000 °C. A magnesium perchlorate trap was used to remove water from the gas stream. Isotopic measurements were standardized against three in-house standards (two glutamic acids "GA1" and "GA2", and dried salmon "SA"), which are calibrated to international reference materials USGS40 and USGS41. An aliquot of the Neoarchean Mt. McRae Shale was analyzed as an in-house standard to test long-term precision. Isotopic data are reported in delta notation relative to air for nitrogen and Vienna PeeDee Belemnite (V-PDB) for carbon.

Analytical blanks resulting from combustion were monitored and subtracted from nitrogen data; blanks were negligible for carbon measurements. Average analytical accuracy of $\delta^{15}N$ among individual runs, based on in-house standard "GA1" was $-0.03 \pm 0.19‰$ ($1\sigma$). Accuracy of $\delta^{13}C_{org}$ measurements based on in-house standard "SA" was $-0.05 \pm 0.07‰$ ($1\sigma$). The average analytical

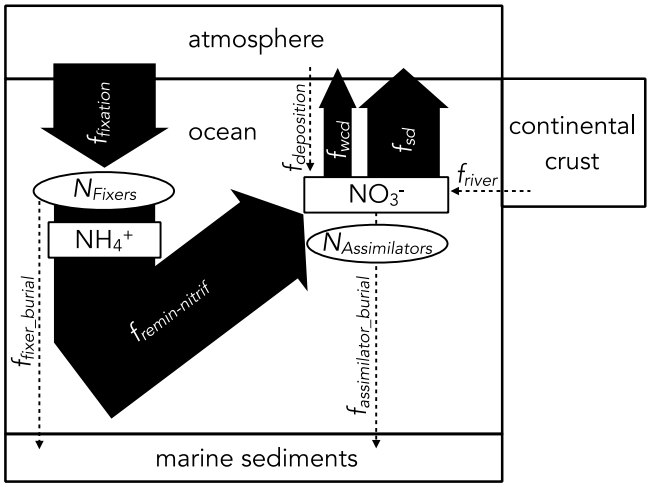


**Fig. 1.** Box model schematic of Earth's surface nitrogen cycle. Nitrogen fixation ($f_{fixation}$) is the dominant input to the ocean system, with water column ($f_{wcd}$) and sediment ($f_{sd}$) denitrification constituting the major output fluxes. The dominant input (>99%) of nitrate is nitrification ($f_{remin\text{-}nitrif}$), with atmospheric deposition ($f_{deposition}$) and riverine ($f_{river}$) inputs comprising only minor contributions (<1%). Modern flux constants were used to calibrate the model, and then the balance of $f_{wcd}$, $f_{sd}$, and $f_{burial}$ (including burial of both fixers and assimilators) was adjusted to simulate changes in ocean redox chemistry. Since remineralization of organic matter produces a small or negligible N isotope fractionation, ammonium burial with clay minerals is not treated separately in the model. A detailed description of model architecture can be found in the Supplementary Materials.

precision among all runs based on in-house standard "UW-McRae" was 0.12‰ ($1\sigma$) for $\delta^{15}N$ and 0.04‰ ($1\sigma$) for $\delta^{13}C_{org}$. All samples were analyzed at least twice, with an average standard deviation between sample replicates of 0.25‰ for $\delta^{15}N$ and 0.17‰ for $\delta^{13}C_{org}$.

Samples from the Sengoma Argillite Formation were analyzed for bulk nitrogen content and $\delta^{15}N_{bulk}$ values (without decarbonation) following standard procedures in the Stable Isotopes for Innovative Research Laboratory at the Department of Geological Sciences, University of Manitoba (cf. Zerkle et al., 2017). Analyses were performed using a Costech$^{TM}$ 4010 Elemental Analyzer coupled to a Thermo Finnigan$^{TM}$ Delta V Plus isotope-ratio mass spectrometer. A magnesium perchlorate-carbosorb trap was placed before ConFlo III to remove water and $CO_2$. Temperature in the oxidation column was raised to 1050 °C for efficient sample combustion, and a 'macro' $O_2$ injection loop was utilized. $CO_2$ levels were monitored during analytical sessions. Sample normalization was performed using two-point calibration with two international standards (USGS40 and USGS41) at the beginning, middle, and end of each run. To monitor the quality of analytical performance, two certified standards were analyzed alongside with samples: B2153, soil, % TN = 0.13 ± 0.02%, $\delta^{15}N = +6.70 \pm 0.15$‰ (Elemental Microanalysis); and SDO-1, Devonian Ohio Shale, % TN = 0.36 ± 0.01%, $\delta^{15}N = -0.8 \pm 0.3$‰ (USGS). The data obtained were TN (wt.%) = 0.14 ± 0.00% and $\delta^{15}N$ values of +6.76 ± 0.02‰ ($n = 3$) for B2153, and TN (wt.%) = 0.37 ± 0.00% and $\delta^{15}N$ values of −0.32 ± 0.02‰ ($n = 3$) for SDO-1.

### 3.4. Isotope box model

We constructed a steady-state box model of the nitrogen cycle to track the salient processes affecting nitrogen isotope mass balance in the ocean system (Fig. 1). The major input of nitrogen to the ocean is biological $N_2$ fixation to $NH_4^+$, which is released during biomass degradation and oxidized rapidly to $NO_3^-$ (nitrification). We assumed that nitrification occurs instantaneously as soon as $NH_4^+$ upwells to the surface ocean, because previous studies have shown that nitrification proceeds even at nanomolar levels of dissolved $O_2$ (e.g. Kalvelage et al., 2011). The major output of nitrogen from the ocean is assumed to be denitrification ($NO_3^-$ reduction to $N_2$), which occurs in suboxic-to-anoxic parts of the water column (here defined as <4.5 μM $O_2$; Keeling et al., 2010) and in anoxic sedimentary porewaters. We did not separately parameterize the anammox pathway ($NH_4^+$ oxidation to $N_2$ using $NO_2^-$) because the isotopic effect is similar to canonical denitrification and thus a changing balance between anammox and canonical denitrification is unlikely to affect the nitrogen isotope mass balance of the ocean (Devol, 2015).

We first calibrated our model to reproduce the isotopic mass balance of the modern ocean (Devol, 2015). Then we adjusted the balance of water column and sedimentary denitrification as a function of anoxia in the ocean. The isotopic composition of export production was calculated for two end-member scenarios: (1) a closed system where nitrate is irreversibly transformed into either $N_2$ (via denitrification) or biomass (via assimilation) (i.e. resulting in progressive isotopic distillation of the residual pool at higher yields), and (2) an open system at steady state (i.e. resulting in isotopic offsets between products and reactants that are nearly identical to the fractionation factor) (cf. Hayes, 2004). Because the residence time of nitrogen in the modern ocean is ~3 kyrs (Brandes and Devol, 2002), nitrogen is moderately well-mixed in the modern open ocean, and thus nitrogen isotope mass balance should generally follow open-system dynamics (as is assumed for carbon isotope mass balance; Hayes, 2004; Schidlowski, 2001). However, in modern basins with very high rates of water column denitrification, the isotopic distillation of residual $NO_3^-$ can locally approach closed system dynamics, causing nitrogen isotope ratios in certain regions of the modern ocean to become substantially elevated above global mean values (Tesdal et al., 2013). In the low-oxygen Precambrian ocean, closed-system behavior of nitrogen isotopes may have been more prevalent, particularly prior to the GOE. Thus, we present both calculations, noting that the open-system scenario more accurately captures the global average value for marine sediments with predominantly oxic environments, while local environments can be susceptible to closed system dynamics. A full description of all parameterizations and equations can be found in the Supplementary Materials.

## 4. Results

### 4.1. Isotopic results

All of the studied units consistently show bulk-rock $\delta^{15}N$ values (Fig. 2; Table S1) that are elevated above the range expected from nitrogen fixation alone (−2‰ to +1‰; Zhang et al., 2014). The mean $\delta^{15}N_{bulk}$ value of all units analyzed is +4.8 ± 1.4‰ ($1\sigma$), which closely resembles the nitrogen isotope composition of modern marine sediments (mode +4‰ to +6‰; Tesdal et al., 2013). Within individual units, $\delta^{15}N_{bulk}$ values are fairly consistent over several meters in stratigraphy, with an average per-unit standard deviation of 0.6‰ (ranging from 0.2‰ to 1.8‰). The full range of $\delta^{15}N_{bulk}$ values in the samples analyzed in this study is +1.1‰ to +7.7‰, which largely overlaps the range seen in modern marine sediments (Tesdal et al., 2013). Notably, we find no evidence of extremely enriched $\delta^{15}N_{bulk}$ values (> +10‰) in any of the units studied here (Fig. 2), which stands in contrast to the data from Paleoproterozoic shales of the Aravalli Supergroup in India (Papineau et al., 2009).

Kerogen isolates were isotopically lighter than their corresponding bulk-rock values by an average of −2.5‰ (Fig. 3; Table S1). The isotopic offset increased as a function of metamorphic grade, with unmetamorphosed samples showing a small positive offset (+0.6‰; $n = 4$), while samples that reached prehnite–pumpellyite

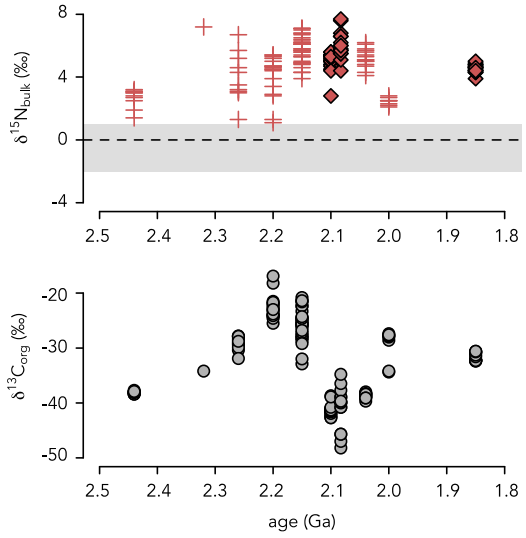


**Fig. 2.** $\delta^{15}N_{bulk}$ (top) and $\delta^{13}$ $C_{org}$ (bottom) values of samples analyzed in this study. Crosses denote nitrogen isotope data from units that experienced lower greenschist facies metamorphism, diamonds denote data from units that remained below greenschist facies. All nitrogen isotope data are enriched above the range of values expected for nitrogen-fixation dominated systems (−2‰ to +1‰; grey shaded region). Most units contain carbon isotope ratios that are depleted below the normal range for marine phytoplankton (−26‰ ± 7‰; Schidlowski, 2001), perhaps reflecting heterotrophic degradation of sedimentary organic matter in anoxic seawater and sediments.

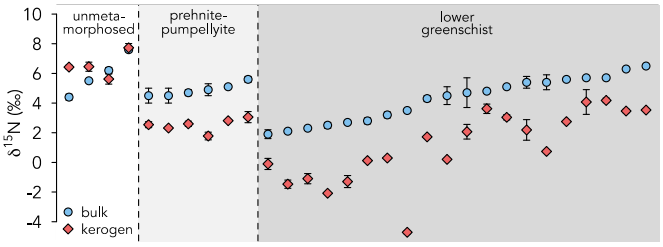


**Fig. 3.** Comparison of $\delta^{15}$ $N_{bulk}$ and $\delta^{15}$ $N_{ker}$ values for individual samples (error bars = 1$\sigma$). The $\delta^{15}N_{ker}$ values show a trend of being consistently isotopically lighter than their corresponding $\delta^{15}N_{bulk}$ values, which is consistent with a previous study (Stüeken et al., 2017). Furthermore, the isotopic offset tends to be larger at higher metamorphic grade, which corroborates the suggestion that isotopic re-equilibration occurs between nitrogen phases under progressive metamorphism. The isotopic offsets observed in the samples are consistent with the metamorphic grades that have been inferred from mineral assemblages.

facies (−2.4‰; $n = 6$) and lower greenschist facies (−3.2‰; $n = 20$) showed a moderate negative offset (Fig. 3).

A LOWESS (LOcally WEighted Scatterplot Smoothing) curve was used to describe variability in the nitrogen isotope record across the GOE (details can be found in Supplementary Materials). Bulk-rock nitrogen isotope data from Precambrian marine sedimentary rocks were compiled from the literature by updating a published database (Stüeken et al., 2016). All published data from units spanning 3.3 to 1.3 Ga were included in the LOWESS calculations. The mean $\delta^{15}N$ value of the LOWESS curve is +3.6 ± 1.2‰ (1$\sigma$). The curve shows a secular trend across the GOE, with $\delta^{15}N$ values rising in the late Archean, reaching a maximum just prior to the GOE, stabilizing across much of the Paleoproterozoic, and slightly decreasing in the Mesoproterozoic (Fig. 9).

The mean $\delta^{13}C_{org}$ value of all samples in our dataset is −32.5 ± 7.3‰ (1$\sigma$). As with $\delta^{15}N$, $\delta^{13}C_{org}$ values for individual units are fairly consistent, with an average per-unit standard deviation of 1.8‰ (ranging from 0.2‰ to 3.9‰). Most studied units contain samples with $\delta^{13}C_{org}$ values that are more negative than the range typically generated by marine phytoplankton (−26‰ ± 7‰; Schidlowski, 2001), which might reflect heterotrophic activity, including methanogenesis, occurring in predominantly anoxic sediments, and methanotrophy either at the sediment–water interface or throughout the overlying water column utilizing dissolved oxidants (e.g. Bekker et al., 2008; Luo et al., 2014). A notable exception is an increase in $\delta^{13}C_{org}$ values seen in units deposited during the ca. 2.22–2.06 Ga Lomagundi carbon isotope excursion (Fig. 2), with $\delta^{13}C_{org}$ values rising to −22.6 ± 2.2‰ (1$\sigma$) in the Wewe Slate and −25.7 ± 3.0‰ (1$\sigma$) in the Sengoma Argillite Formation (Bekker et al., 2008).

### 4.2. Model outputs

The box model-estimated mean $\delta^{15}N$ value for modern marine sediments (assuming open-system dynamics) is +4.5‰, with a confidence interval of +2.6‰ to +7.3‰ based on uncertainties in fractionation factors for nitrogen fixation and water column denitrification. The closed system approach yields similar results (mean = +5.5‰, range of +3.5‰ to +8.5‰). Both approaches thus accurately capture the average composition of modern marine sediments (mode +4–6‰ ± 2.5‰; Tesdal et al., 2013).

As the relative proportion of suboxic-to-anoxic ocean water increases beyond modern values and approaches 100% (i.e. $p_{an+sub}$ approaches 100), sedimentary $\delta^{15}N$ values first increase due to enhanced water column denitrification, but ultimately decline toward the "$N_2$-fixation window" (−2‰ to +1‰) in strongly anoxic oceans (Fig. 8) because the rate of nitrogen removal is so rapid (and nearly quantitative) that nitrogen-fixing rather than nitrate-assimilating organisms dominate the nitrogen isotope mass-balance (cf. Fennel et al., 2005). In the closed system model, values do not return to the "$N_2$-fixation window" even in fully anoxic oceans ($f_{an+sub} = 100$), because the extremely fractionated nitrate associated with a totally closed system would still drive sedimentary $\delta^{15}N$ values to become positive even with a minimal biomass contribution from nitrate-assimilating organisms. However, such extreme fractionations are unlikely to have occurred, since the ocean cannot be a totally closed system (i.e. nitrogen is continually being fixed into biomass and made bioavailable through remineralization and nitrification). Reality for the full range of ocean redox states thus lies somewhere between the two endmembers captured by the separate calculations.

## 5. Discussion

### 5.1. Preservation of primary isotopic signals

Before using nitrogen isotopes in ancient marine sedimentary rocks to reconstruct paleoenvironmental conditions, it must be demonstrated on a case-by-case basis that the observed isotopic signatures indeed reflect the primary cycling of nitrogen in the ocean at the time of deposition (Ader et al., 2016). This screening draws first from consideration of nitrogen cycling in the modern ocean. The nitrogen isotopic composition of modern marine sediments faithfully records the $\delta^{15}N$ value of biomass exported from the photic zone (Altabet and Francois, 1994), which is an admixture of nitrogen-fixing and nitrogen-assimilating organisms. Planktonic biomass in the modern ocean has an average molar C/N ratio of ∼7 (Redfield, 1934), and the remineralization of biomass in the water-column and sediments can increase the C/N values preserved in marine sediments. The C/N values of our samples predominantly fall between 5 and 100 (Fig. 4), which is consistent with moderate diagenetic reworking of primary biomass. The Timeball Hill Formation has several samples with C/N values <5 (Fig. 4), which suggests either (a) trapping of nitrogen in clay minerals during diagenesis, while carbon was oxidized and lost from the system, or (b) post-depositional introduction of non-primary

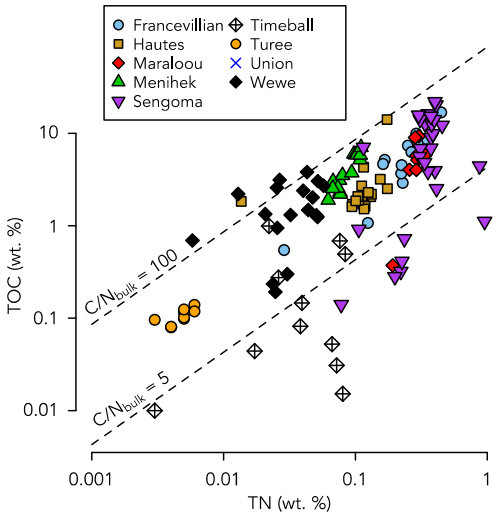


**Fig. 4.** Total organic carbon versus total nitrogen values for all bulk-rock measurements in this study. Dotted lines show C/N ratios of 5 and 100, respectively. The average molar C/N ratio of planktonic biomass in the modern ocean is ~7 (Redfield, 1934). Water-column and sedimentary diagenesis can increase sedimentary C/N ratios, giving a spread in values similar to what is observed in most units in this study. Causes for low sedimentary C/N ratios are discussed in Section 5.1 of the main text.

nitrogen (perhaps via hydrothermal fluids). As discussed below, the fact that kerogen extracts from these samples show expected isotopic offsets is consistent with a primary biomass origin for the nitrogen in these samples, as was suggested by Luo et al. (2018).

Diagenesis can modify the $\delta^{15}N$ values of organic matter in marine sediments, but this effect is typically much smaller than the fractionations imparted during nitrogen cycling in the water column. In oxic sediments, the remineralization of organic-bound nitrogen can leave residual biomass isotopically heavier by 1.4–2.3‰ (Lehmann et al., 2002; Möbius, 2013). However, the effect is smaller under anoxic conditions (Lehmann et al., 2002), which likely prevailed in Precambrian marine sedimentary environments. Thus, while the precise contribution of diagenesis is difficult to assess, the isotopic effect of diagenesis on the $\delta^{15}N$ values was probably minor ($<1$‰) compared to the magnitude of the isotopic enrichment ($\gg 1$‰) seen in these samples.

After diagenesis, nitrogen isotope ratios can be further modified during metamorphism. This involves two types of isotopic effects: isotopic partitioning between kerogen- and mineral-bound nitrogen within the bulk rock (Stüeken et al., 2017) and loss of nitrogen out of the bulk rock (Bebout and Fogel, 1992; Haendel et al., 1986). While the isotopic partitioning between nitrogen phases within a bulk-rock sample can be significant (3–4‰) at low metamorphic grades (Stüeken et al., 2017), the effect of nitrogen loss on bulk-rock $\delta^{15}N$ values is typically small in units that have remained below greenschist-facies metamorphism ($<1$‰) or even within greenschist facies (1–2‰; Rivera et al., 2015). The finding that $\delta^{15}N_{ker}$ values are systematically depleted (on average by $-2.5$‰) relative to corresponding $\delta^{15}N_{bulk}$ values in this dataset is consistent with previous studies of metamorphic effects on nitrogen isotope partitioning (Stüeken et al., 2017). Furthermore, the increase in isotopic offset from near-zero in unmetamorphosed samples to ~3‰ in lower greenschist facies samples (Fig. 3) is in good agreement with a systematic survey of metamorphic effects on sedimentary $\delta^{15}N$ values (Stüeken et al., 2017). Thus, we follow Stüeken et al. (2017) in taking $\delta^{15}N_{bulk}$ values as a more robust indicator of primary $\delta^{15}N$ values in these samples.

In cases where metamorphism has significantly altered bulk-rock nitrogen isotope ratios, it has been shown that progressive metamorphism causes preferential loss of nitrogen relative to carbon, and of $^{14}N$ relative to $^{15}N$ (Bebout and Fogel, 1992). Thus, a positive correlation between $\delta^{15}N_{bulk}$ and C/N ratios can be indicative of metamorphic alteration of bulk-rock nitrogen isotope ratios, and a positive correlation between $\delta^{15}N_{bulk}$ and $\delta^{13}C_{org}$ would suggest that both nitrogen and carbon isotopes were affected by metamorphism. There are no such positive correlations observed across our entire dataset (Fig. 5) or within individual units (Figs. S1 and S2), including those that reached greenschist facies metamorphism. The effect of metamorphism on the bulk-rock nitrogen and organic carbon isotope ratios in these samples was therefore probably minor, meaning that the trends in nitrogen and carbon isotopes seen across the GOE are primary isotopic signals indicative of environmental conditions at the time of deposition.

### 5.2. Interpretation of isotopic data

#### 5.2.1. Mechanisms for generating positive $\delta^{15}N$ values

There are multiple ways to generate positive $\delta^{15}N$ values in ancient marine sedimentary rocks (see Ader et al., 2016; Stüeken et al., 2016). These mechanisms all pertain to the cycling of nitrogen after biological $N_2$ fixation, which imparts only a small fractionation under most conditions ($-2$‰ to $+1$‰; Zhang et al., 2014). Under conditions of replete dissolved Fe supply this fractionation can be slightly larger, generating biomass that is depleted by as much as $-4$‰ relative to atmospheric nitrogen (Zerkle et al., 2008). However, the lack of fairly negative $\delta^{15}N$ values in

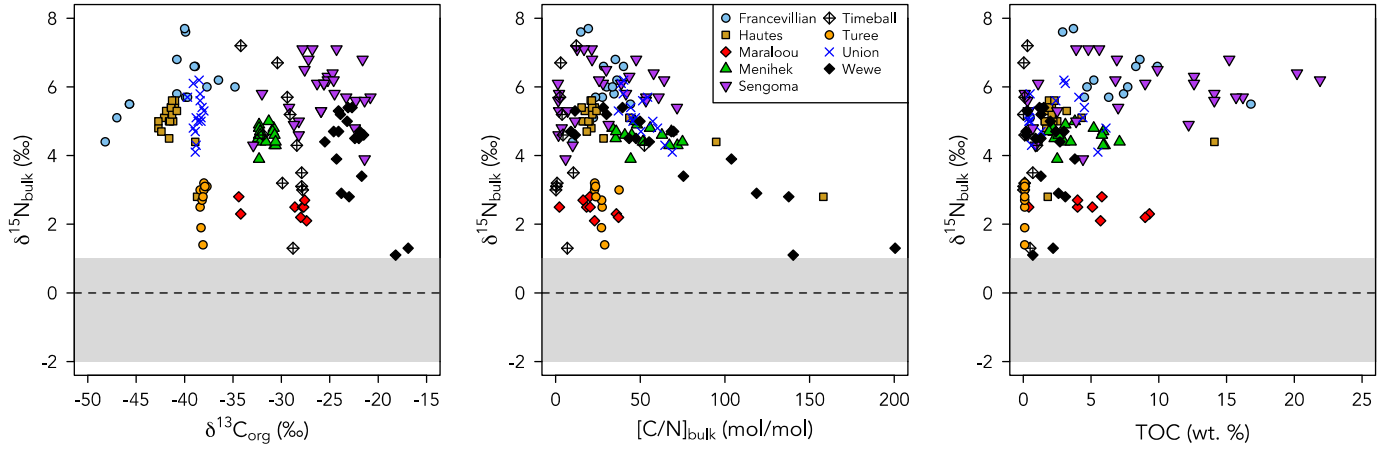


**Fig. 5.** Cross-plot assessment of the preservation of primary nitrogen isotope ratios. Grey shaded region denotes $\delta^{15}N_{bulk}$ values associated with nitrogen fixation-dominated ecosystems. The lack of co-variation between $\delta^{15}N_{bulk}$ and $\delta^{13}C_{org}$, C/N, and TOC suggests that the $\delta^{15}N_{bulk}$ values were not strongly affected by diagenetic and metamorphic overprinting. See discussion for further details and Figs. S1–S3 for plots of individual units.

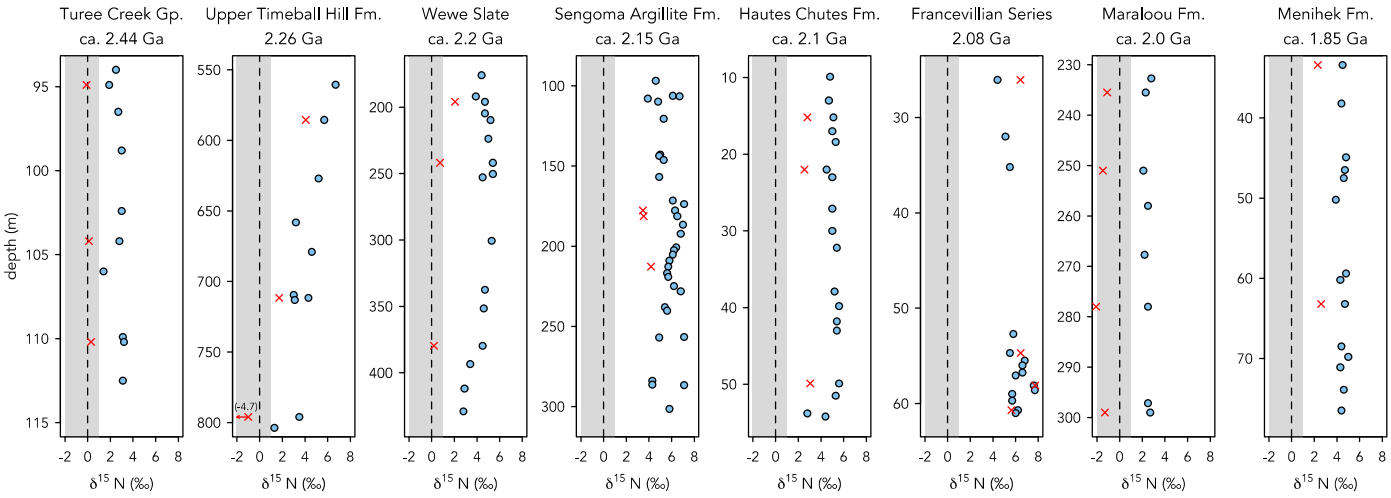


**Fig. 6.** Nitrogen isotope values plotted along stratigraphic profiles. Circles show bulk-rock data, crosses denote kerogen isolates. All studied units show $\delta^{15}N_{bulk}$ values that are consistently above the values expected for a fully anaerobic, fixation-dominated ecosystem (grey shaded region). Outcrop samples from the Union Island Group are not plotted as they were collected from multiple outcrops.

the Precambrian rock record – even in environments that are thought to have been ferruginous and dominated by $N_2$ fixation – suggests that these extreme conditions were not representative of global nitrogen cycling (Koehler et al., 2017; Stüeken, 2013; Stüeken et al., 2015).

As discussed in Section 5.1, the release of nitrogen during remineralization of organic matter imparts a negligible fractionation, making it unlikely to explain an isotopic enrichment of several permil. However, the re-assimilation of ammonium ($NH_4^+$) generated during remineralization can impart a large isotopic fractionation (up to −27‰) if the process is non-quantitative, with biomass becoming isotopically light (Hoch et al., 1992). Such a mechanism has been proposed to explain the very large spread of $\delta^{15}N$ values seen in shales of the late Paleoproterozoic Aravalli Supergroup (Papineau et al., 2009). This mechanism would require that non-quantitative $NH_4^+$ assimilation created a pool of isotopically light biomass and drove the isotopic composition of residual $NH_4^+$ isotopically heavy. The transport of the heavy nitrogen to another site and subsequent quantitative assimilation could plausibly generate elevated $\delta^{15}N$ values in marine sediments. However, the absence of isotopically light nitrogen in the nine units studied here makes this explanation seem unlikely. Furthermore, even in modern redox-stratified marine basins, such as the Black Sea, the accumulation of appreciable dissolved $NH_4^+$ does not correlate with isotopic evidence of partial assimilation (e.g. Fulton et al., 2012). Sediments underlying these modern anoxic waters have $\delta^{15}N$ values near 0‰, suggestive of nitrogen fixation in the photic zone followed by quantitative uptake of liberated $NH_4^+$. This can be attributed to the fact that nitrogen is the limiting nutrient in the ocean on short, Ka-timescales (Tyrrell, 1999), and thus uptake of bioavailable nitrogen in the photic zone is typically quantitative.

While nitrogen uptake into biomass tends to have no net isotopic effect, partial removal of bioavailable nitrogen from the ocean through redox processes can result in significant isotopic fractionations. One such pathway is the nitrification of $NH_4^+$ into $NO_3^-$, which – if non-quantitative – can create a $NO_3^-$ pool that is isotopically light and leave a residual, heavy pool of $NH_4^+$ (Casciotti et al., 2003). The resulting biomass could become isotopically heavy if organisms quantitatively assimilate the heavy $NH_4^+$, while the light $NO_3^-$ is quantitatively removed via denitrification to the atmosphere (Thomazo et al., 2011). However, it is unlikely that this sort of system would have been stable on geological timescales. Today, partial nitrification is only observed in regions of the modern ocean where seasonal redox-stratification occurs (e.g. Granger et al., 2011). This is because nitrification is rapid, and can even proceed at nanomolar levels of dissolved oxygen (e.g. Kalvelage et al., 2011). Furthermore, the same conditions that would favor non-quantitative nitrification (seasonally variable redox-stratification) might be inimical to quantitative denitrification, as the latter process is not as rapid, and rarely goes to completion in the open ocean (Devol, 2015).

Another explanation for isotopic enrichment in marine settings is non-quantitative denitrification occurring in suboxic regions of the open ocean. This process imparts a large isotopic fractionation (−10 to −30‰; Devol, 2015; Kritee et al., 2012), causing residual dissolved $NO_3^-$ to become isotopically heavy ($\delta^{15}N > 0$‰). Importantly, denitrification occurring in sedimentary porewaters nearly goes to completion, resulting in a flux of isotopically heavy nitrogen from the ocean back into the atmosphere, counterbalancing the isotopically light flux from suboxic waters. The quantitative assimilation of the residual heavy $NO_3^-$ then records the net isotopic distillation of the reservoir imparted by denitrification, which ultimately gets preserved in marine sediments. This mechanism is thought to control the isotopic mass balance of the modern ocean system (Devol, 2015), causing the $\delta^{15}N$ values of most modern marine sediments to fall between +4‰ and +6‰ (Tesdal et al., 2013).

Considering all possible mechanisms listed above, the positive $\delta^{15}N$ values seen in the Paleoproterozoic units studied here are most compellingly explained by similar processes to those operating in the modern ocean: rapid nitrification, non-quantitative denitrification in suboxic regions of the water column, and quantitative assimilation of residual $NO_3^-$ in the photic zone. In other words, our nitrogen isotope data suggest that an aerobic nitrogen cycle persisted across continental shelves between about 2.44 and 1.85 Ga.

### 5.2.2. Aerobic nitrogen cycling in the early Paleoproterozoic

While transient excursions to elevated $\delta^{15}N$ values – indicative of local aerobic nitrogen cycling – have been observed in Neoarchean shales (Garvin et al., 2009; Koehler et al., 2018), it remains unclear to what extent these settings are representative of global redox conditions at that time. The large isotopic variability seen in some Neoarchean facies is consistent with a small $NO_3^-$ reservoir (Garvin et al., 2009; Koehler et al., 2018), which could promote substantial inter-basinal variability and closed-system dynamics (discussed further in Section 5.3). In contrast, the more stable stratigraphic $\delta^{15}N$ profiles of the Paleoproterozoic (Fig. 6)

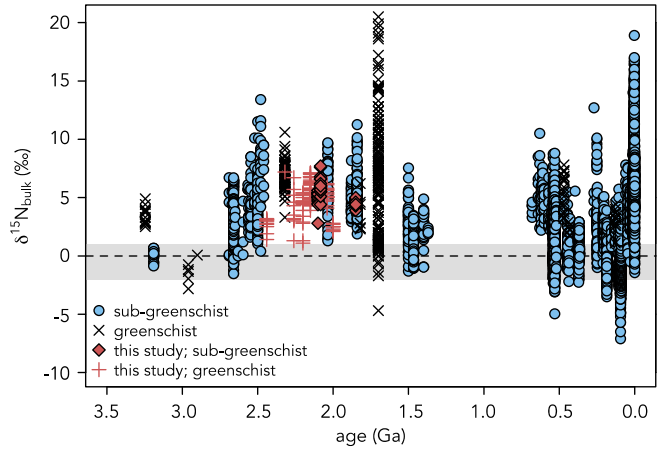


**Fig. 7.** Bulk-rock $\delta^{15}N$ values of marine sedimentary rocks through geologic time. Consistently positive $\delta^{15}N$ values in Paleoproterozoic shales imply that oxic conditions were prevalent in surface waters for hundreds of millions of years after the onset of the Great Oxidation Event. Published data and references can be found in the Supplementary Materials.

may reflect growth of the $NO_3^-$ reservoir, with the ocean residence time of $NO_3^-$ becoming sufficiently long that relatively rapid and large-magnitude isotopic excursions are not seen within continuous lithostratigraphic units. This was first suggested by Zerkle et al. (2017), who found evidence of aerobic nitrogen cycling in the early stages of the GOE in the 2.32 Ga Lower Timeball Hill Formation of the Pretoria Group in South Africa, and further confirmed by the findings of another recent study of multiple drill cores in the Pretoria Group (Luo et al., 2018). Our dataset corroborates those findings, showing instances of elevated $\delta^{15}N$ values in the Upper Timeball Hill Formation. Additionally, we find that shales of the ca. 2.44 Ga Turee Creek Group in Western Australia, which were deposited shortly before the onset of the GOE, have $\delta^{15}N$ values (ranging from +2‰ to +3‰) that are consistent with a minor, but persistent, contribution of aerobic nitrogen cycling to the isotopic composition of preserved biomass. However, because diagenetic and metamorphic overprinting could have potentially contributed a post-depositional enrichment of $\delta^{15}N_{bulk}$ values by ~1–2‰, it is difficult to use the Turee Creek data to precisely gauge the extent of aerobic nitrogen cycling immediately prior to the GOE.

The state of the nitrogen cycle appears to have been fairly stable across the GOE and the proposed "oxygen overshoot" during the Lomagundi carbon isotope excursion (ca. 2.22–2.06 Ga; Bekker and Holland, 2012). Even in the aftermath of the GOE (i.e. after ca. 2.06 Ga), when sulfur and selenium isotope records point to a contraction of oxygenated seawater (Planavsky et al., 2012; Scott et al., 2014; Kipp et al., 2017), nitrogen isotopes continue to record aerobic nitrogen cycling in the surface ocean (Fig. 7). This is unlikely to be an artifact of poor age constraints and low sample density – many of the nitrogen isotope data are from the same units that were used to argue for waxing and waning marine oxygen levels across the GOE based on molybdenum (Scott et al., 2008) and uranium (Partin et al., 2013) enrichments, multiple sulfur isotopes (Scott et al., 2014), and selenium enrichments and isotope ratios (Kipp et al., 2017). Instead, the differential response of these redox proxies may be indicative of the mechanism by which the Earth transitioned from the "oxygen overshoot" interval to the apparently oxygen-limited mid-Proterozoic.

The record of sedimentary enrichments of redox-sensitive elements is influenced by both the rate of continental oxidative weathering, which supplies them to the ocean, and the areal extent of anoxic and euxinic marine sediments, which efficiently scavenge redox-sensitive elements from the water column. The sharp peak in redox-sensitive trace element enrichments between 2.32 Ga and 2.06 Ga is thus suggestive of both vigorous oxidative weathering and an expansion of at least mildly oxygenated waters at the expense of anoxic and euxinic settings (Partin et al., 2013; Kipp et al., 2017). The size of the marine sulfate reservoir is sensitive to the same conditions, and correspondingly shows a similar trend, as inferred from both carbonate-associated sulfate (Planavsky et al., 2012) and multiple sulfur isotope data from sedimentary sulfides (Scott et al., 2014). In contrast, sedimentary nitrogen isotope ratios reflect the balance between nitrogen fixation and assimilation of dissolved $NO_3^-$ (the isotopic composition of the latter being predominantly set by rates of denitrification) in the part of the water column where primary productivity is the highest, i.e. the photic zone. Unlike sulfur and trace metals, $NO_3^-$ is largely produced within the ocean via nitrification and thus to a first order is independent from oxidative weathering. The persistence of isotopic evidence for $NO_3^-$ uptake after the proposed "oxygen overshoot" interval therefore suggests that the photic zone on continental shelves remained at least mildly oxygenated in the aftermath of the GOE, while the areal extent of anoxic marine sediments increased.

This aerobic state of the nitrogen cycle has not persisted uninterrupted since the GOE. In the Mesoproterozoic, basinal gradients in $\delta^{15}N$ values have been observed, with near-shore facies recording aerobic nitrogen cycling, while offshore facies reflect quantitative assimilation and nitrogen fixation (Stüeken, 2013; Koehler et al., 2017). Our dataset samples only relatively deep-water environments, so we cannot speak to basinal $\delta^{15}N$ gradients within any of the units studied here. However, the persistence of elevated $\delta^{15}N$ values in these settings during and after the GOE demonstrates that aerobic nitrogen cycling prevailed even on the outer shelf. With the available data we are unable to precisely constrain the time at which basinal gradients became representative of the global nitrogen cycle. However, some insight into this matter is offered by the youngest unit in our dataset, the ca. 1.85 Ga Menihek Formation of the Superior Craton in Canada. The positive $\delta^{15}N$ values (+3.9 to +5.0‰) and small isotopic variability ($1\sigma = 0.3$‰) in this unit are both consistent with a significant contribution of aerobic nitrogen cycling and a large bioavailable $NO_3^-$ reservoir in offshore environments in this basin. Thus, this unit might provide a maximum age for the transition to the basinal stratification observed in the Mesoproterozoic nitrogen isotope record.

### 5.3. Quantifying the relationship between ocean oxygenation and nitrogen cycling

While a qualitative interpretation of this dataset yields a compelling story about the oxygenation of the surface ocean in the early Paleoproterozoic, more information can be gleaned by considering these data in a quantitative framework. Our model outputs (Fig. 8) show that under pervasive anoxia ($p_{an\text{-}sub}$ approaching 100%), sedimentary $\delta^{15}N$ values approach the "$N_2$ fixation window" (−2‰ to +1‰), which indicates that assimilation of $NO_3^-$ into biomass becomes negligible due to increasing denitrification rates. Under these conditions, the majority of marine biomass is comprised of either $N_2$-fixing organisms or $NH_4^+$ assimilating organisms (which were not explicitly tracked in the model). In either case, $NO_3^-$, which is the preferred nitrogenous compound utilized by eukaryotes in the modern ocean (Karl et al., 2001), is rapidly removed via water column denitrification in strongly anoxic oceans, preventing $NO_3^-$ assimilators from contributing substantially to sedimentary export production (cf. Fennel et al., 2005).

These results suggest that the persistence of a stable, isotopically recordable $NO_3^-$ reservoir requires perhaps as much as ~90% of the surface ocean to be at least mildly oxygenated (Fig. 8). Precisely what concentration of dissolved $O_2$ defines "mildly oxygenated" is unresolved by this model; for the purpose of this

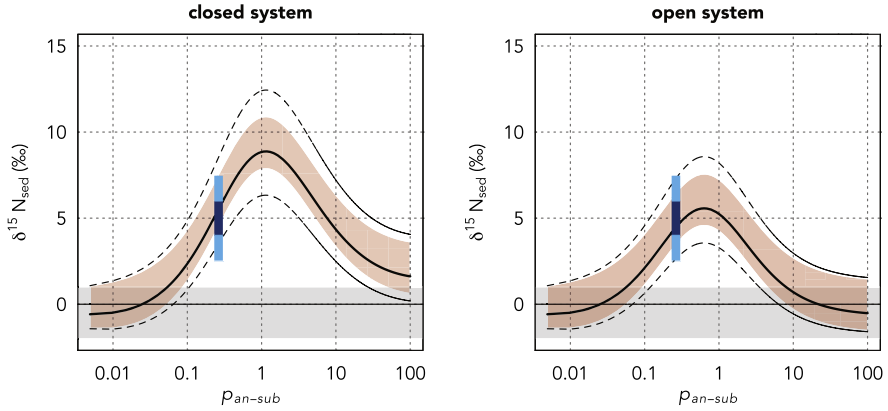


**Fig. 8.** Modeled bulk-rock sedimentary $\delta^{15}$N values under closed (left) and open (right) system dynamics, as a function of anoxia-to-suboxia extent ($p_{an\text{-}sub}$) in the upper ocean. Anoxia-to-suboxia is defined here as seawater with <4.5 μM of dissolved $O_2$ (see Supplementary Materials for discussion), where $p_{an\text{-}sub} = 100$ corresponds to a globally anoxic ocean, and the modern ocean has a $p_{an\text{-}sub}$ value of 0.3. The mode in the $\delta^{15}$N values of modern marine sediments is shown with a dark-blue bar (Tesdal et al., 2013); the lighter-blue bar corresponds to the 1$\sigma$ range. Red-shaded region shows uncertainty interval derived from the range of isotopic fractionations associated with biological $N_2$-fixation. Black dashed lines show cumulative uncertainty interval including upper and lower limits on net isotopic effect of water column denitrification. Grey band denotes isotopic range of nitrogen fixation-dominated ecosystems. (For interpretation of the colors in the figure(s), the reader is referred to the web version of this article.)

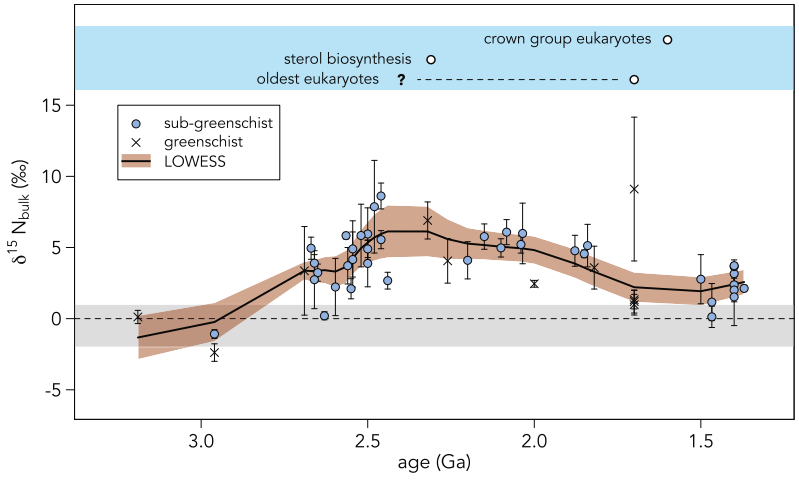


**Fig. 9.** Archean and Paleoproterozoic nitrogen isotope record and constraints on early eukaryotic evolution. Points are mean $\delta^{15}$N values for individual formations with 1$\sigma$ error bars. Black line is LOWESS curve, with 1$\sigma$ confidence interval shown in red shaded region. LOWESS calculations utilized a $d$ value of 1 (local fits via linear regression) and an $f$ value of 0.3 in order to investigate long-term ($\sim 10^8$ yr) trends. References for evolutionary events are discussed in Section 5.4 of the text.

discussion, we are referring to the $O_2$ level at which nitrification outpaces denitrification, thereby allowing the accumulation of a bioavailable nitrate reservoir. In our model scenarios we dictated that the switch to denitrifying conditions occurs when dissolved $O_2$ falls below 4.5 μM (meaning that higher levels would constitute "mildly oxygenated" waters) because the majority of water column denitrification occurs in these settings in the modern ocean (Codispoti et al., 2001; Keeling et al., 2010; Paulmier and Ruiz-Pino, 2009). However, it is known that denitrification can occur at dissolved $O_2$ levels of >20 μM (Kalvelage et al., 2011) and previous modeling has suggested that denitrification outpaces nitrification until dissolved $O_2$ exceeds 11 μM (Fennel et al., 2005). Regardless of precisely where this threshold lies, the persistence of aerobic nitrogen cycling across much of the Paleoproterozoic suggests that the threshold was exceeded in the surface waters of most basins for a few hundred million years following the GOE.

This is a particularly important consideration when addressing the meaning of elevated $\delta^{15}$N values in Neoarchean versus Paleoproterozoic marine sedimentary rocks. In studies of Neoarchean units, large deviations from the "$N_2$ fixation window" towards elevated values have been interpreted as indicating transient oxygenation in the water column prior to the GOE (Garvin et al., 2009; Koehler et al., 2018). The Neoarchean basins in which these trends were observed most likely conformed to closed system dynamics rather than the open-system dynamics that characterize nitrogen isotope mass balance in the modern ocean, because the $NO_3^-$ was sourced locally in the upper water column and was unlikely to become well-mixed in such a strongly anoxic ocean. With this being the case, further studies that increase spatial resolution of the nitrogen isotope record in the potentially heterogeneous Neoarchean ocean could help determine whether the positive $\delta^{15}$N values in those strata record local or global redox fluctuations.

### 5.4. Implications for primary productivity and the emergence of eukaryotic ecosystems

Before the GOE, it is thought that a scarcity of phosphorus restricted rates of primary productivity (Bekker and Holland, 2012; Kipp and Stüeken, 2017; Reinhard et al., 2016). The lack of sufficient oxidizing power may have inhibited the recycling of organic-bound phosphorus within the ocean until marine dissolved oxygen and sulfate levels rose in the Paleoproterozoic (Planavsky et al., 2012; Scott et al., 2014), implying that the total rate of carbon recycling and net primary productivity could have increased in tan-

dem with the oxygenation of the Earth's surface environments (cf. Bekker and Holland, 2012). It is conceivable that an increase in phosphorus availability during the GOE (cf. Bekker and Holland, 2012) could have caused nitrogen to become the limiting nutrient in the marine environment. However, the data presented here, as well as those presented in previous studies of nitrogen isotopes in Paleoproterozoic marine sedimentary rocks (Godfrey et al., 2013; Kump et al., 2011; Luo et al., 2018; Papineau et al., 2009; Zerkle et al., 2017), show no evidence of persistent nitrogen limitation on geological timescales after the onset of the GOE. Quite to the contrary, the persistence of elevated nitrogen isotope ratios in Paleoproterozoic shales suggests that fixed nitrogen was sufficiently available to fuel primary production (discussed in Section 5.2.1). Still, while nitrogen was likely not limiting, it is not entirely clear whether it was phosphorus, trace metals, or some other factor that controlled the rate of primary productivity during the Lomagundi carbon isotope excursion and associated "oxygen overshoot" interval, which is thought to have been a time of extreme organic carbon burial (Bekker and Holland, 2012; Karhu and Holland, 1996).

A further question is whether these more productive, nitrate-fueled ecosystems contained eukaryotic organisms. Considerable controversy surrounds the oldest evidence of eukaryotes; it is generally accepted that the eukaryotic lineage had emerged by ca. 1.7 Ga (see Javaux and Lepot, 2018), though arguments for an earlier arrival of eukaryotes are not lacking (e.g. Bengtson et al., 2017; El Albani et al., 2010). Notably, a recent genomic effort to resolve the origin of sterol biosynthesis has suggested that this metabolic capacity – a hallmark of eukaryotic organisms – evolved nearly contemporaneously with the onset of the GOE (Gold et al., 2017). However, the record of organic biomarkers in Proterozoic sedimentary successions implies that eukaryotes were not significant contributors to bulk organic matter until the late Neoproterozoic (Brocks et al., 2017). While efforts to confidently constrain when the eukaryotes first evolved and reached abundance in the sedimentary record will carry on, geochemical constraints will be critical to answering fundamental questions about the interplay between environmental changes and biological responses.

The data presented here have two implications for early eukaryotic evolution. First, the prevalence of elevated $\delta^{15}N$ values in the early Paleoproterozoic (Figs. 7, 9) is direct evidence of abundant $NO_3^-$ assimilating organisms. Whether a substantial portion of this biomass was comprised of eukaryotes is unclear from the nitrogen isotope data alone, but this trend in nitrogen isotopes confirms that $NO_3^-$ was sufficiently bioavailable across continental shelves to alleviate any fixed-nitrogen limitation on eukaryotic proliferation at this time (Fig. 9). Second, the magnitude of nitrogen isotope enrichment and consistency of values, when viewed in the context of our model outputs, imply that much of the photic zone overlying continental shelves was at least mildly oxygenated for hundreds of millions of years in the Paleoproterozoic. Thus, if they had already evolved, eukaryotes with oxygen-requiring metabolic processes should have been able to persist in the upper part of the water column without severe oxygen-limitation. Still, it remains plausible that periodic incursions of anoxic waters and redox fluctuations at low dissolved $O_2$ levels could have restricted the proliferation and diversification of eukaryotes at this time (cf. Johnston et al., 2012). In any case, the data presented here allow for an earlier emergence of eukaryotes than is deemed likely under recent interpretations of the fossil and biomarker records (Fig. 9).

## 6. Conclusion

We have presented new nitrogen isotope data spanning the Paleoproterozoic Era that document persistent aerobic nitrogen cycling on continental shelves from ca. 2.44 to 1.85 Ga. The observation that nitrogen isotope ratios remain elevated when trace metal and sulfur-based proxies point to a decrease in the extent of oxic settings following the ca. 2.32–2.06 Ga "oxygen overshoot" may derive from the fact that the latter proxies are sensitive to redox conditions at the sediment–water interface, while nitrogen isotope values record redox conditions in the photic zone. When viewed in light of our model outputs, these data implicate oxygenated surface seawater and substantial bioavailable $NO_3^-$ lasting from the onset of the GOE until at least ca. 1.85 Ga. This may suggest that the upper ocean was already hospitable to eukaryotic organisms hundreds of millions of years before the fossil record firmly indicates their presence.

## Acknowledgements

We thank Andy Schauer and the UW IsoLab for technical support. MAK acknowledges support from NSF Graduate Research Fellowship DGE-1256082. AB acknowledges funding from NSERC Discovery and Accelerator grants. Funding for isotopic analyses was provided by the UW Department of Earth & Space Sciences to MAK and by NASA Exobiology grant NNX16AI37G to RB. We thank Vincent Busigny and one anonymous reviewer for comments that substantially improved this work, as well as Derek Vance for editorial handling.

## Appendix A. Supplementary material

Supplementary material related to this article can be found online at https://doi.org/10.1016/j.epsl.2018.08.007.

## References

Ader, M., Thomazo, C., Sansjofre, P., Busigny, V., Papineau, D., Laffont, R., Cartigny, P., Halverson, G.P., 2016. Interpretation of the nitrogen isotopic composition of Precambrian sedimentary rocks: assumptions and perspectives. Chem. Geol. 429, 93–110.

Altabet, M.A., Francois, R., 1994. Sedimentary nitrogen isotopic ratio as a recorder for surface ocean nitrate utilization. Glob. Biogeochem. Cycles 8, 103–116.

Bebout, G.E., Fogel, M.L., 1992. Nitrogen-isotope compositions of metasedimentary rocks in the Catalina Schist, California: implications for metamorphic devolatilization history. Geochim. Cosmochim. Acta 56, 2839–2849.

Bekker, A., Holland, H.D., 2012. Oxygen overshoot and recovery during the early Paleoproterozoic. Earth Planet. Sci. Lett. 317, 295–304. https://doi.org/10.1016/j.epsl.2011.12.012.

Bekker, A., Holland, H.D., Wang, P.-L., Rumble, D., Stein, H.J., Hannah, J.L., Coetzee, L.L., Beukes, N.J., 2004. Dating the rise of atmospheric oxygen. Nature 427, 117–120.

Bekker, A., Holmden, C., Beukes, N.J., Kenig, F., Eglinton, B., Patterson, W.P., 2008. Fractionation between inorganic and organic carbon during the Lomagundi (2.22–2.1 Ga) carbon isotope excursion. Earth Planet. Sci. Lett. 271, 278–291.

Bengtson, S., Rasmussen, B., Ivarsson, M., Muhling, J., Broman, C., Marone, F., Stampanoni, M., Bekker, A., 2017. Fungus-like mycelial fossils in 2.4-billion-year-old vesicular basalt. Nat. Ecol. Evol. 1, 0141.

Beukes, N.J., Dorland, H., Gutzmer, J., Nedachi, M., Ohmoto, H., 2002. Tropical laterites, life on land, and the history of atmospheric oxygen in the Paleoproterozoic. Geology 30, 491–494.

Brandes, J.A., Devol, A.H., 2002. A global marine-fixed nitrogen isotopic budget: implications for Holocene nitrogen cycling. Glob. Biogeochem. Cycles 16.

Brocks, J.J., Jarrett, A.J., Sirantoine, E., Hallmann, C., Hoshino, Y., Liyanage, T., 2017. The rise of algae in Cryogenian oceans and the emergence of animals. Nature 548, 578.

Casciotti, K.L., Sigman, D.M., Ward, B.B., 2003. Linking diversity and stable isotope fractionation in ammonia-oxidizing bacteria. Geomicrobiol. J. 20, 335–353.

Codispoti, L.A., Brandes, J.A., Christensen, J.P., Devol, A.H., Naqvi, S.W.A., Paerl, H.W., Yoshinari, T., 2001. The oceanic fixed nitrogen and nitrous oxide budgets: moving targets as we enter the anthropocene? Sci. Mar. 65, 85–105.

Devol, A.H., 2015. Denitrification, anammox, and $N_2$ production in marine sediments. Annu. Rev. Mar. Sci. 7, 403–423.

El Albani, A., Bengtson, S., Canfield, D.E., Bekker, A., Macchiarelli, R., Mazurier, A., Hammarlund, E.U., Boulvais, P., Dupuy, J.-J., Fontaine, C., Fürsich, F.T., Gauthier-Lafaye, F., Janvier, P., Javaux, E., Ossa, F.O., Pierson-Wickmann, A.-C., Riboulleau, A., Sardini, P., Vachard, D., Whitehouse, M., Meunier, A., 2010. Large colonial organisms with coordinated growth in oxygenated environments 2.1 Gyr ago. Nature 466, 100–104. https://doi.org/10.1038/nature09166.

Farquhar, J., Bao, H.M., Thiemens, M., 2000. Atmospheric influence of Earth's earliest sulfur cycle. Science 289, 756–758. https://doi.org/10.1126/science.289.5480.756.

Fennel, K., Follows, M., Falkowski, P.G., 2005. The co-evolution of the nitrogen, carbon and oxygen cycles in the Proterozoic ocean. Am. J. Sci. 305, 526–545.

Fulton, J.M., Arthur, M.A., Freeman, K.H., 2012. Black Sea nitrogen cycling and the preservation of phytoplankton $\delta^{15}N$ signals during the Holocene. Glob. Biogeochem. Cycles 26.

Garvin, J., Buick, R., Anbar, A.D., Arnold, G.L., Kaufman, A.J., 2009. Isotopic evidence for an aerobic nitrogen cycle in the latest Archean. Science 323, 1045–1048.

Godfrey, L.V., Poulton, S.W., Bebout, G.E., Fralick, P.W., 2013. Stability of the nitrogen cycle during development of sulfidic water in the redox-stratified late Paleoproterozoic Ocean. Geology 41, 655–658.

Gold, D.A., Caron, A., Fournier, G.P., Summons, R.E., 2017. Paleoproterozoic sterol biosynthesis and the rise of oxygen. Nature 543, 420–423.

Granger, J., Prokopenko, M.G., Sigman, D.M., Mordy, C.W., Morse, Z.M., Morales, L.V., Sambrotto, R.N., Plessen, B., 2011. Coupled nitrification–denitrification in sediment of the eastern Bering Sea shelf leads to $^{15}N$ enrichment of fixed N in shelf waters. J. Geophys. Res., Oceans 116.

Gumsley, A.P., Chamberlain, K.R., Bleeker, W., Söderlund, U., de Kock, M.O., Larsson, E.R., Bekker, A., 2017. Timing and tempo of the Great Oxidation Event. Proc. Natl. Acad. Sci. USA 114, 1811–1816. https://doi.org/10.1073/pnas.1608824114.

Haendel, D., Mühle, K., Nitzsche, H.-M., Stiehl, G., Wand, U., 1986. Isotopic variations of the fixed nitrogen in metamorphic rocks. Geochim. Cosmochim. Acta 50, 749–758.

Hardisty, D.S., Lu, Z., Bekker, A., Diamond, C.W., Gill, B.C., Jiang, G., Kah, L.C., Knoll, A.H., Loyd, S.J., Osburn, M.R., et al., 2017. Perspectives on Proterozoic surface ocean redox from iodine contents in ancient and recent carbonate. Earth Planet. Sci. Lett. 463, 159–170.

Hayes, J.M., 2004. An Introduction to Isotopic Calculations. Woods Hole Oceanogr. Inst., Woods Hole, MA.

Hoch, M.P., Fogel, M.L., Kirchman, D.L., 1992. Isotope fractionation associated with ammonium uptake by a marine bacterium. Limnol. Oceanogr. 37, 1447–1459.

Javaux, E., Lepot, K., 2018. The Paleoproterozoic fossil record: implications for the evolution of the biosphere during Earth's middle-age. Earth-Sci. Rev. 176, 68–86.

Johnston, D.T., Poulton, S.W., Goldberg, T., Sergeev, V.N., Podkovyrov, V., Vorob'eva, N.G., Bekker, A., Knoll, A.H., 2012. Late Ediacaran redox stability and metazoan evolution. Earth Planet. Sci. Lett. 335, 25–35. https://doi.org/10.1016/j.epsl.2012.05.010.

Kalvelage, T., Jensen, M.M., Contreras, S., Revsbech, N.P., Lam, P., Günter, M., LaRoche, J., Lavik, G., Kuypers, M.M.M., 2011. Oxygen sensitivity of anammox and coupled N-cycle processes in oxygen minimum zones. PLoS ONE 6, e29299. https://doi.org/10.1371/journal.pone.0029299.

Karhu, J.A., Holland, H.D., 1996. Carbon isotopes and the rise of atmospheric oxygen. Geology 24, 867–870.

Karl, D.M., Bidigare, R.R., Letelier, R.M., 2001. Long-term changes in plankton community structure and productivity in the North Pacific Subtropical Gyre: the domain shift hypothesis. Deep Sea Res., Part II, Top. Stud. Oceanogr. 48, 1449–1470.

Keeling, R.F., Körtzinger, A., Gruber, N., 2010. Ocean deoxygenation in a warming world. Annu. Rev. Mar. Sci. 2, 199–229.

Kipp, M.A., Stüeken, E.E., 2017. Biomass recycling and Earth's early phosphorus cycle. Sci. Adv. 3, eaao4795.

Kipp, M.A., Stüeken, E.E., Bekker, A., Buick, R., 2017. Selenium isotopes record extensive marine suboxia during the Great Oxidation Event. Proc. Natl. Acad. Sci. USA 114, 875–880. https://doi.org/10.1073/pnas.1615867114.

Koehler, M.C., Buick, R., Kipp, M.A., Stüeken, E.E., Zaloumis, J., 2018. Transient surface ocean oxygenation recorded in the ~2.66 Ga Jeerinah Formation, Australia. Proc. Natl. Acad. Sci. USA 115 (30), 7711–7716. https://doi.org/10.1073/pnas.1720820115.

Koehler, M.C., Stüeken, E.E., Kipp, M.A., Buick, R., Knoll, A.H., 2017. Spatial and temporal trends in Precambrian nitrogen cycling: a Mesoproterozoic offshore nitrate minimum. Geochim. Cosmochim. Acta 198, 315–337.

Kritee, K., Sigman, D.M., Granger, J., Ward, B.B., Jayakumar, A., Deutsch, C., 2012. Reduced isotope fractionation by denitrification under conditions relevant to the ocean. Geochim. Cosmochim. Acta 92, 243–259.

Kump, L.R., Junium, C., Arthur, M.A., Brasier, A., Fallick, A., Melezhik, V., Lepland, A., Črne, A.E., Luo, G., 2011. Isotopic evidence for massive oxidation of organic matter following the Great Oxidation Event. Science 334, 1694–1696. https://doi.org/10.1126/science.1213999.

Lehmann, M.F., Bernasconi, S.M., Barbieri, A., McKenzie, J.A., 2002. Preservation of organic matter and alteration of its carbon and nitrogen isotope composition during simulated and in situ early sedimentary diagenesis. Geochim. Cosmochim. Acta 66, 3573–3584.

Luo, G., Junium, C.K., Izon, G., Ono, S., Beukes, N.J., Algeo, T.J., Cui, Y., Xie, S., Summons, R.E., 2018. Nitrogen fixation sustained productivity in the wake of the Palaeoproterozoic Great Oxygenation Event. Nat. Commun. 9, 978.

Luo, G., Junium, C.K., Kump, L.R., Huang, J., Li, C., Feng, Q., Shi, X., Bai, X., Xie, S., 2014. Shallow stratification prevailed for 1700 to 1300 Ma ocean: evidence from organic carbon isotopes in the North China Craton. Earth Planet. Sci. Lett. 400, 219–232.

Luo, G., Ono, S., Beukes, N.J., Wang, D.T., Xie, S., Summons, R.E., 2016. Rapid oxygenation of Earth's atmosphere 2.33 billion years ago. Sci. Adv. 2, e1600134. https://doi.org/10.1126/sciadv.1600134.

Lyons, T.W., Reinhard, C.T., Planavsky, N.J., 2014. The rise of oxygen in Earth's early ocean and atmosphere. Nature 506, 307–315. https://doi.org/10.1038/nature13068.

Möbius, J., 2013. Isotope fractionation during nitrogen remineralization (ammonification): implications for nitrogen isotope biogeochemistry. Geochim. Cosmochim. Acta 105, 422–432.

Papineau, D., Purohit, R., Goldberg, T., Pi, D., Shields, G.A., Bhu, H., Steele, A., Fogel, M.L., 2009. High primary productivity and nitrogen cycling after the Paleoproterozoic phosphogenic event in the Aravalli Supergroup, India. Precambrian Res. 171, 37–56.

Partin, C.A., Bekker, A., Planavsky, N.J., Scott, C.T., Gill, B.C., Li, C., Podkovyrov, V., Maslov, A., Konhauser, K.O., Lalonde, S.V., Love, G.D., Poulton, S.W., Lyons, T.W., 2013. Large-scale fluctuations in Precambrian atmospheric and oceanic oxygen levels from the record of U in shales. Earth Planet. Sci. Lett. 369, 284–293. https://doi.org/10.1016/j.epsl.2013.03.031.

Paulmier, A., Ruiz-Pino, D., 2009. Oxygen minimum zones (OMZs) in the modern ocean. Prog. Oceanogr. 80, 113–128.

Planavsky, N.J., Bekker, A., Hofmann, A., Owens, J.D., Lyons, T.W., 2012. Sulfur record of rising and falling marine oxygen and sulfate levels during the Lomagundi event. Proc. Natl. Acad. Sci. USA 109, 18300–18305. https://doi.org/10.1073/pnas.1120387109.

Redfield, A.C., 1934. On the proportions of organic derivatives in sea water and their relation to the composition of plankton. In: James Johnstone Memorial Volume, pp. 176–192.

Reinhard, C.T., Planavsky, N.J., Gill, B.C., Ozaki, K., Robbins, L.J., Lyons, T.W., Fischer, W.W., Wang, C., Cole, D.B., Konhauser, K.O., 2016. Evolution of the global phosphorus cycle. Nature 541, 386–389. https://doi.org/10.1038/nature20772.

Rivera, K.T., Puckette, J., Quan, T.M., 2015. Evaluation of redox versus thermal maturity controls on $\delta^{15}N$ in organic rich shales: a case study of the Woodford Shale, Anadarko Basin, Oklahoma, USA. Org. Geochem. 83, 127–139.

Schidlowski, M., 2001. Carbon isotopes as biogeochemical recorders of life over 3.8 Ga of Earth history: evolution of a concept. Precambrian Res. 106, 117–134.

Scott, C., Lyons, T.W., Bekker, A., Shen, Y., Poulton, S.W., Chu, X., Anbar, A.D., 2008. Tracing the stepwise oxygenation of the Proterozoic ocean. Nature 452, 456–459. https://doi.org/10.1038/nature06811.

Scott, C., Wing, B.A., Bekker, A., Planavsky, N.J., Medvedev, P., Bates, S.M., Yun, M., Lyons, T.W., 2014. Pyrite multiple-sulfur isotope evidence for rapid expansion and contraction of the early Paleoproterozoic seawater sulfate reservoir. Earth Planet. Sci. Lett. 389, 95–104. https://doi.org/10.1016/j.epsl.2013.12.010.

Stüeken, E.E., 2013. A test of the nitrogen-limitation hypothesis for retarded eukaryote radiation: nitrogen isotopes across a Mesoproterozoic basinal profile. Geochim. Cosmochim. Acta 120, 121–139. https://doi.org/10.1016/j.gca.2013.06.002.

Stüeken, E.E., Buick, R., Guy, B.M., Koehler, M.C., 2015. Isotopic evidence for biological nitrogen fixation by molybdenum-nitrogenase from 3.2 Gyr. Nature 520, 666–669. https://doi.org/10.1038/nature14180.

Stüeken, E.E., Kipp, M.A., Koehler, M.C., Buick, R., 2016. The evolution of Earth's biogeochemical nitrogen cycle. Earth-Sci. Rev. 160, 220–239.

Stüeken, E.E., Zaloumis, J., Meixnerová, J., Buick, R., 2017. Differential metamorphic effects on nitrogen isotopes in kerogen extracts and bulk rocks. Geochim. Cosmochim. Acta 217, 80–94. https://doi.org/10.1016/j.gca.2017.08.019.

Tesdal, J.-E., Galbraith, E.D., Kienast, M., 2013. Nitrogen isotopes in bulk marine sediment: linking seafloor observations with subseafloor records. Biogeosciences 10, 101–118. https://doi.org/10.5194/bg-10-101-2013.

Thomazo, C., Ader, M., Philippot, P., 2011. Extreme $^{15}N$-enrichments in 2.72-Gyr-old sediments: evidence for a turning point in the nitrogen cycle. Geobiology 9, 107–120.

Tyrrell, T., 1999. The relative influences of nitrogen and phosphorus on oceanic primary production. Nature 400, 525–531.

Zerkle, A.L., Junium, C.K., Canfield, D.E., House, C.H., 2008. Production of $^{15}N$-depleted biomass during cyanobacterial $N_2$-fixation at high Fe concentrations. J. Geophys. Res., Biogeosci. 113, G03014. https://doi.org/10.1029/2007JG000651.

Zerkle, A.L., Poulton, S.W., Newton, R.J., Mettam, C., Claire, M.W., Bekker, A., Junium, C.K., 2017. Onset of the aerobic nitrogen cycle during the Great Oxidation Event. Nature 543, 465–467.

Zhang, X., Sigman, D.M., Morel, F.M., Kraepiel, A.M., 2014. Nitrogen isotope fractionation by alternative nitrogenases and past ocean anoxia. Proc. Natl. Acad. Sci. USA 111, 4782–4787.